CERN/SPSC 85-44
SPSC/I 160
31 July 1985

LETTER OF INTENT

STUDY OF NUCLEON STRUCTURE FUNCTIONS FROM NUCLEI UP TO AND BEYOND THE KINEMATICAL LIMIT

S.P. Baranov[2], D.Yu. Bardin[1], J. Cvach[1], V.Kh. Dodokhov[1], A.V. Efremov[1], N.G. Fadeev[1], V. Genchev[1], I.A. Golutvin[1], V.F. Grushin[2], J. Hladky[1], V.Yu. Karzhavin[1], M.Yu. Kazarinov[1], V.S. Khabarov[1], Yu.T. Kiryushin[1], V.S. Kisselev[1], A.A. Komar[2], I.G. Kosarev[1], V.G. Krivokhizhin[1], V.V. Kukhtin[1], R. Lednicky[1], W. Lohmann[1], V.N. Lysyakov[1], S. Nemecek[1], Yu.A. Panebratsev[1], P. Reimer[1], I.A. Savin[1], N.B. Skachkov[1], A.I. Semenyushkin[1], A.A. Shikanjan[2], G.I. Smirnov[1], D.A. Smolin[1], J. Strakhota[1], G. Sultanov[1], E.V. Telyukov[2], P. Todorov[1], A.V. Vishnevsky[1], N.V. Vlasov[1], A.G. Volodko[1], A.V. Zarubin[1], N.I. Zamyatin[1]

[1] Joint Institute for Nuclear Research, Dubna

[2] Lebedev Physical Institute, Academy of Science USSR, Moscow

Abstract

We propose to perform an experiment on deep inelastic muon-nucleon scattering with the purpose to study the x-dependence of nucleon structure functions and their ratios in the range of Q^2 = 50-200 GeV^2 and x = 0.4-2.0. Such measurements performed on a number of nuclei with atomic weights from 2 to 207 would provide new information for detailed studies of the EMC effect and tests of many models explaining the x-behaviour of the nucleon structure functions and their ratios. The measurements will be decisive for the proof that a quark-parton model of a nucleus adequately describes nuclear structure probed at high energies.

The upgraded high luminocity BCDMS spectrometer with improved resolution in transfered energy ν will be used for measurements. We request 280 or 200 GeV muon beam with a total of $3 \cdot 10^{13}$ muons (200 days).

TABLE OF CONTENTS

INTRODUCTION

As is well known investigation of deep inelastic scattering (DIS) of leptons on nucleons and nuclei in the range of 4-momentum transfers Q^2 *) up to 200 GeV^2 yielded an extremely valuable information on nucleon structure and scaling violation hypothesis. There were also obtained important results demonstrating the existence of nuclear effects in the x-behaviour of nucleon structure functions (EMC effect). Unfortunately high energy muon and neutrino experiments have been carried out in a rather limited range of Bjorken variable x below $x = 0.7$. The data that can be obtained in the range $x > 0.7$ can not be considered only as complementary to those already obtained in the low x region. They are essential for accurate determination of the QCD parameter Λ and are expected to be decisive for understanding of a quark-parton picture of a nucleus.

We therefore propose to carry out dedicated measurements of nuclear structure functions in high x range that is out of the reach for present high energy DIS experiments.

Three principal points of such a study are listed below.

i) Study of the x-dependence of a nucleon structure functions in the region $0.4 < x < 1.0$ and of its sensitivity to an atomic weight A and Q^2 in the range $A = 2$-207 and $Q^2 = 50$-200 GeV^2.

ii) Measurement of the x-dependence of nucleon structure functions on deuterium and iron nuclei up to the highest possible x, tentatively up to $x = 2$ for iron and $x = 1.5$ for deuterium.

iii) Study of the x-dependence of the ratio of iron to deuterium structure functions in the range up to $x = 1.5$.

---

*) We use standard notations for kinematical variables of muon-nucleon DIS: $E(E')$, $P(P')$ and $\Theta(\theta')$ are the energy, momentum and the angle of incident (scattered) lepton, M is a nucleon mass, $Q^2 = 4EE' \sin^2(\theta'/2)$, $\nu = E-E'$, $x = Q^2/2M\nu$.

All the measurements can be performed with the BCDMS set up[1] after minor modifications. We are going to exploit the main advantages of the existing apparatus: a) high luminocity, b) high and flat acceptance at large Q^2 and x and c) selective Q^2 and x trigger. A principal change in the set up will be the addition of an hadron calorimeter to measure an energy of hadrons produced in DIS.

The programme of measurements including calibrations and data taking needs two years starting from 1986.

2. PHYSICS MOTIVATIONS

2.1. Nucleon Structure Functions Near Kinematical Limit $x = 1$

Discovery of EMC effect [2] has tought us that a number of features of deep inelastic scattering of leptons on nuclei can be very important in understanding nuclear structure. There has been developed a number of theoretical models describing the EMC effect. Most of them [3,4] explain the effect inside the explored kinematic range but can be critically tested only outside the region of performed measurements. It is quite natural therefore to extend now investigations in the range of Bjorken variable x where either no or only poor information on structure functions is available. First of all it is small-x region, that is going to be studied at CERN thoroughly in an experiment proposed recently [5]. The region of large x is going to be investigated in the framework of present proposal. It should be noted that single nucleon kinematics allows for $x_{max} = 1$. Calculating Bjorken x for nuclear targets we shall use $M = 1$ instead of $M = A$. Then for the kinematic limit on a nucleus we obtain $x_{max} = A$. Estimates of x-dependence of structure functions for $x > 1$ are strongly model-dependent but it is clear, that for present muon and neutrino beams the region beyond $x=2$ remains unaccessible due to statistical limitations.

European Muon Collaboration (EMC) has demonstrated in 1983 that there exists a difference in the x-dependence of nucleon

structure functions measured on free nucleons and on those bound in nuclei. It has been found also that nuclear medium does not affect the Q^2-dependence of structure functions. The ratio of structure functions measured on iron and deuterium and integrated over Q^2-range is shown in fig.1. The same result has been obtained in 1984 by Bolonga-CERN-Dubna-Munich-Saclay (BCDMS) collaboration /6/. BCDMS has also measured the ratio of nitrogen to deuterium structure functions (fig.2) that is also sensitive to binding effects. The results of SLAC measurements carried out with an electron beam at transfered momenta Q^2 by order of magnitude smaller are shown for comparison /7/. They also indicate that Q^2-dependence of effect (at least within the range of medium x) is negligible. On the other hand SLAC results can not be considered as precise since the ratio R of longitudinal (σ_L) to transverse (σ_T) virtual photon absorbtion cross sections poorly known in the region of small Q^2 and x can significantly modify the x-dependence of structure functions /8/.

The discovery of the EMC came as a surprise to many theorists. But soon enough there were proposed several models explaining the effect. Though they are sometimes very different they are united by the idea that the standard picture of nuclear structure considering a nucleus as a system of bound nucleons is not enough accurate. Indeed if the momentum transfer from a muon to a nucleus is large enough ($\gtrsim$1 GeV/c) the latter has to be considered as a relativistic bound state of a quantized fields, i.e. as a system with infinite degrees of freedom. The "valence" nucleons of the system carry only a part of its total momentum (in the infinite momentum frame of reference). The rest have to belong to a particle-antiparticle "sea" (mesons, quarks, gluons) due to vacuum polarization effect (production and absorbtion of virtual particles). This results in the decrease of the fraction of momentum of valence quarks in the nucleus (per a nucleon) and in the increase of the fraction of momentum of sea quarks and gluons. These general features of the relativistic bound state are common to all models proposed for explanation of the EMC effect. For instance, one assumes in some of them:

a) An increase of the size of nucleons in a nucleus [9] or an increase of the colour confinment radius in a nucleus [10] that leads to softening of valence quark spectrum and consequently brings about the increase of the sea of quark-antiquark pairs and/or gluons.

b) An admixture of Δ -isobars [11] that results in the same effect due to softer valence quark distribution in Δ -resonance.

c) An increase of density of pions surrounding a nucleon in a nucleus [12] that on one hand means an increase of sea quark density and on the other hand means a decrease of momentum fraction related to nucleons or softening of valence quark distribution.

d) Existence of multi-quark configurations [13-16] inside a nucleus that are considered as a transition state between hadronic matter and a quark-gluon plasma. Such states are responsible for th redistribution of valence quarks from medium x-range to the range $x>1$, that brings about the decrease in mean x and the increase of sea quarks and gluons contribution to the total momentum carried by nucleon constituents.

All these and many other models [3,4] suggested for explanation of the EMC effect demonstrate qualitative agreement in the range of $x<0.7$ where experimental data on F_2^A/F_2^D ratios have been already obtained by the EMC and BCDMS collaborations. On the other hand predictions of the models for x above 0.7 (so far unexplored except at SLAC) differ considerably (fig.3). We therefore propose to extend measurements of the ratios of structure functions to the range $x>0.7$.

Measurements of nucleon structure functions alone in the range $0.7<x<1.0$ is of interest from the point of view of determination of the QCD parameter Λ . First of all according to [17] the amount of scaling violation of the nonsinglet structure function observed in the range $0.3<x<0.5$, is controlled by the size of the structure function in the region $x>0.6$. Secondly it is well established fact that the sea quarks and gluons contribution to the range $0.5<x<1.0$ is negligible. This provides better condi-

tions for the determination both the shape of valence quarks distribution and the parameter Λ .

An important information on the nature of EMC effect can be obtained by means of investigation of A-dependence in a wide range of atomic weights. Such measurements have been first carried out by the groupe /7/ at SLAC in deep inelastic electron-nuclei scattering. It has been found that the depletion in F_2^A/F_2^D grows approximately like log A and is the strongest at $x \approx 0.65$. The results of SLAC on the A-dependence of cross sections ratios at $x = 0.3$ and 0.62 along with those obtained by the BCDMS in deep inelastic scattering of muons on deuterium, nitrogen and iron are shown in fig.4. It is of importance to obtain results on A-dependence of F_2^A/F_2^D ratio in $x \approx 1$ region. Such results might help to understand whether Fermi-motion of nucleons at high x or few nucleon correlations /18/ or some other nuclear effects are responsible for the observed rise in the ratio σ^A/σ^D at $x > 0.7$. We propose to carry out measurements on deuterium and on such nuclei as N_2, Al, Fe, Sn, Pb. The set up that is going to be used makes it possible to collect data simultaneously on two targets.

2.2. NUCLEAR STRUCTURE FUNCTIONS BEYOND SINGLE NUCLEON KINEMATIC LIMIT $X = 1$

As has been mentioned already the kinematical limit $x = 1$ for deep inelastic scattering of a muon on a free nucleon becomes $x = A$ if the scattering occurs on a nuclei. That means that the nucleon structure function $F_2(x)$ has nonzero values at $x > 1$. Since nuclear medium can be to a great extent responsible for the shape of nucleon structure function beyond $x = 1$ it is reasonable to introduce the term of "nuclear structure function" $F_2^A(x)$. This region unexplored so far in deep inelastic lepton-nuclei scattering experiments is the subject to be investigated in the framework of the present proposal.

It is reasonable to assume that the EMC effect is closely related to phenomena occurring at x beyond 1. So the models explaining the EMC effect can be tested after data on nuclear structure functions are obtained in a wider range of x. Many of the

models however consider a nucleon Fermi-motion alone to be responsible for nonzero values of nuclear structure function $F_2^A(x)$ at $x>1$. In such a case $F_2^A(x)$ must be very small (practically zero) at $x \approx 1.2$ (dashed line in fig.5). If an evidence for nonzero $F_2^A(x)$ was found at larger x it would witness in favour of the few-nucleon correlations model /18/ and those of multi-quark configurations /13-16/.

The idea of multi-quark configurations in a nucleus can be considered as the development of the idea of the "fluctons" /19/ or short time fluctuations of nuclear matter. Such a hypothesis proved to be useful in explaining high emission rate of light nuclei (d, t, α) produced in collisions of fast protons with heavy nuclei. Later the idea took a form of "few nucleon correlations"/18/ and "multi-quark fluctons"/20/ in explaining cumulative hadron production in hadron nuclei collisions. Hadrons emitted far beyond single nucleon kinematic limit have been called cumulative ones.

A special approach /21/ has been developed justifying the use of experimental information on cumulative hadron production for the study of quark distributions in nuclei. Its essential assumption is the requirement of the limiting fragmentation cross section of a nucleus to mesons to be proportional to the nuclear quark-parton structure function in a way like this occurs for the deep inelastic lepton-nuclei scattering. This in turn can be justified if one considers quarks as quasi-free particles in a nucleus.

Experiments on limiting fragmentation of a nucleus already a long time provide exciting data on nuclear structure /22-24/. Even if one can argue on the validity of such an approximation, one can not deny good qualitative agreement between the results obtained in deep inelastic lepton scattering experiments and those obtained earlier in experiments on limiting fragmentation of nuclei. Fig. 6 for example shows the results on the ratio of inclusive hadron production cross sections interpreted in terms of structure functions. Common features observed in hadron and lepton experiments in the range $x<1$ is an indication of validity of the approach /21/. It also seems reasonable to regard the results obtained by nuclear physicists in the range $x>1$ as a good indication of

manifestation of the quark-parton structure of a nucleus.

Below we present a list of principal features of nuclear structure functions as they have been obtained experimentally /25/.

1. Nuclear quark-parton structure function is greater than 0 up to $x = 3$.

2. Nuclear structure function of medium and heavy nuclei can be fit by an exponential $a \cdot \exp(-x/b)$ with $b = 0.14$.

3. The ratio F_2^{Pb}/F_2^D is well above unity in the range $1<x<2$. (fig.6).

4. At $x>1$ for nuclei heavier than Al the ratio of structure functions to that of measured on Pb is practically unity (fig.7).

An attempt has been already made by the BCDMS collaboration to observe some of these features in deep inelastic muon scattering on carbon /26/. We took advantage of the fact that geometrical efficiency of the NA-4 set up does not decrease when x rises. In a period from 1979 to 1980 many data on carbon target have been obtained in the range of x close to unity that in principle could provide high statistical accuracy. Unfortunately large smearing with respect to x makes it practically impossible to analyse the data in a model independent way that results in considerable systematic errors. To take into account smearing effects in the data analysis there has been used a model with an exponential structure function $F_2 \sim \exp(-x/b)$, with $b = 0.16$. As a result the structure function (fig.8) integrated over Q^2 has been obtained. It is well fit by an exponential with the parameter $b = 0.14 \pm 0.01$ (stat.) /26/. This preliminary result is nevertheless a proof of possibility of investigation of nuclear structure functions provided the resolution with respect to x is improved.

Though experiments on limiting fragmentation of nuclei look very promising for the study of nuclear structure especially in the range of x as high as 2-3, there remains an open question whether multiquark configurations exist in nuclei or they are created by incident hadron. Results on structure functions

measured in deep inelastic muon-nuclei scattering in the range of x beyond unity will give definite answer to this question.

Poor resolution with respect to x has been so far main obstacle in deep inelastic scattering experiments to reach good precision in the range $x > 0.7$. The following relation

$$x = \frac{Q^2}{2M\nu} \simeq \frac{E_0}{M}\theta'^2\left(\frac{E_0}{\nu} - 1\right)$$

holds true in the kinematic range of the proposed measurements. Then the accuracy in Bjorken x can be expressed as

$$\frac{\Delta x}{x} = \left[\left(2\frac{\Delta\theta'}{\theta'}\right)^2 + k^2\left(\frac{\Delta\nu}{\nu}\right)^2\right]^{\frac{1}{2}},$$

where $k = \frac{E_0/\nu}{E/\nu - 1}$.

High accuracy in the measurement of the scattered muon angle can be reached quite easily (except very small angles) and is of order 3% for the front set up of the BCDMS spectrometer /1/. The resolution with respect to x is particularly low in the range of low ν where the resolution $\Delta\nu/\nu$ is by order of magnitude worse than that of $\Delta\theta'/\theta'$. Here lies principal limitation of all the experiments on deep inelastic muon and neutrino scattering in reaching the range above $x = 0.7$. So main purpose of modification of the BCDMS spectrometer is the increase of precision in measurement of transfered energy $\nu = E - E'$.

3. PROPOSED MEASUREMENTS

The experimental set up that will suit the purpose of the proposed measurements is the BCDMS spectrometer shown in fig.9 that will be equipped with an hadron calorimeter. A calorimeter is going to be installed in place of the first supermodule. It will measure energy of showers produced in interactions on the target modules of the front set up. Kinematic range that will be covered by such set up is shown in fig.10 by the area shaded with vertical lines. The geometrical acceptance of the apparatus in this region is typically 80% and practically flat for $Q^2 > 50$ GeV^2. The range of studies is extended to larger than

100 mrad angles by registering the events from the target modules inside the iron toroids but with lower accuracy of measured transfered energy.

3.1. Data Taking on D_2, N_2 and Al Targets

The BCDMS spectrometer is usually triggered by the muons that traverse more than 10 m of its standard part accepting thus low x events (fig.11). We consider it necessary to modify the triggering system to bring down events rate from the low x region. Since $x \sim P_T \theta'/\nu$ and P_T is proportional to the track length of a muon oscillating in the magnetic spectrometer the new trigger could be realized by rejection of short track events or those with high ν. Fig.11 demonstrates the decrease by a factor of 8 in the events rate ($x < 0.4$) achieved by the requirement for muons to traverse 12 planes of ring trigger counters instead of 4 planes. The selectivity of the P_T trigger obtained by simulation is shown in fig.12.

The available hardware /1/ makes it possible to realize 8 plains trigger in the fast first-level triggering system. Further reduction in the events rate can be achieved by the second-level trigger using already available hardware. It will be realized first of all by the selection of longer tracks (up to 12 planes of trigger counters). Secondly the events with shorter tracks will be accepted if they are recognized as high Q^2 events (hits in rings beginning from number 4 and hits in outer mosaic trigger counters). Final validation of an event will be realized by means of memory ORs logic.

Estimating expected number of events in the range of $x > 0.5$ we relied upon already available data from the NA-4 set up rather than on theoretical expectations. Fig. 11 demonstrates the distribution of events versus x registered from two front target modules filled with deuterium. The distribution along the target axis is shown in fig. 13. This data sample corresponds to scattered muon angles $\theta' > 40$ mrad where reconstruction accuracy is high. If we take for estimations the maximum muon flux 3.5×10^7/spil

and 70% efficiency of performance both of SPS and the BCDMS spectrometer then one can expect 25000 events in the range $x > 0.5$ in 60 days running on deuterium. We suppose to accumulate even higher statistics on a nitrogen and somewhat smaller on the aluminium target (see Table 1).

As for the range close to $x = 1$ both theoretical and experimental estimates can not be considered as reliable, first due to model uncertainties and secondly due to smearing effects. We can mention however, that models based on a quark-parton picture of a nucleus predict for the fluxes presented in Table 1 hundreds of events in the range $x > 0.8$. The statistical accuracy that can be reached in measurements of the ratio of nitrogen to deuterium structure functions is shown in fig.14. Systematic errors will be discussed in the chapter 4.

3.2. Measurements with Heavy Active Targets (Fe, Sn, and Pb)

Three targets will be performed as a calorimeter modules with 20 mm thick iron and stannum plates and 10 mm thick lead plates. The total thickness will be 630 g/cm^2, 580 g/cm^2 and 970 g/cm^2 correspondingly. One calorimeter module with iron plates will be installed permanently in the beam. First half of this module will be used as a reference target, so that data taking will always take place on two targets simulteneously. This allows minimization of systematic errors and also accumulation of high statistics on an iron target in the range beyond $x = 1$. For estimates of the statistical errors shown in fig. 5 we took the exponential form of the structure function $F_2(x) = a\exp(-x/b)$ with $b = 0.105$ as has been obtained in [27] below $x = 1$. It is evident that even higher statistics can be reached if the $F_2(x)$ follows the exponential law with $b = 0.12$ [28] or $b = 0.14$ [26]. After the shape of the nuclear structure function on iron is determined it will be possible to obtain structure functions on Sn and Pb practically with the same accuracy in shorter time because major contribution to the errors comes from systematics.

Running time is presented in Table 1.

We are going to use data obtained on light and heavy targets to estimate whether nucleon Fermi motion or other nuclear effects prevail in the range $x \approx 1$. If the effect of Fermi motion dominates it will show up in a sharp depletion of a nuclear structure function above $x = 1.2$ for all nuclei.

3.3. Beam Request

In total we request $3 \cdot 10^{13}$ beam muons. We can run at energy 280 GeV in parallel with the team /5/ which submitted the proposal p210 to the SPSC. On the other hand we prefer 200 GeV muon beam. The measurements could start in 1986.

4. MODIFICATIONS OF THE SET UP

The suggested by the present proposal modification of the BCDMS spectrometer will considerably improve resolution with respect to the transfered energy ν and consequently x at minimal expences. Only front part of the set up called a "small angle spectrometer" /1/ will be modified. The toroidal iron spectrometer /29/ will be left intact except the first supermodule that will be removed to provide space for the hadron calorimeter.

4.1. The Hadron Calorimeter

The small angle spectrometer equiped with the hadron calorimeter is shown in fig. 15. The calorimeter that is under construction now will contain about 400 modules with the cross section 15×15 cm^2. Each module is a sandwich made of 40 iron plates 2 cm thick and plastic scintillator plates 1 cm thick. One PM tube registers light collected by a wavelength shifter. The calculated energy resolution can be described as $\sigma(E)/E = 0.8/E^{0.5}$.

Scattered muon angles will be determined by five hexagonal multiwire proportional chambers (HMWPC) 1.5 m diameter. Three target modules shown in fig. 15 are supposed to be used in runs with deuterium or nitrogen. While the acceptance of the BCDMS spectrometer for a certain range of scattered muon angles is practically constant along the target length (see fig.13) the acceptance of the calorimeter falls off with the distance from the vertex. The calorimeter acceptance calculated by means of Monte-Carlo is shown in fig. 16. We can in principle run with all the target modules (including those in the toroids) filled with deuterium (nitrogen). Though the measurements of a hadron shower energy for last 5 modules will not be possible the data can be usefull for the range $x < 0.8$ where the spectrometer resolution can be computed reliably by means of Monte-Carlo.

4.2. Live Targets

Three targets made of Fe, Sn and Pb will perform as calorimeters at the same time. The iron target is designed in the same way as a calorimeter module except that light is collected to 10 PM tubes (see fig.17) for determination of an interaction point with a 6 cm accuracy. This provides a certain improvement of the spectrometer resolution. When insensitive to beam muons such a target can operate at beam fluxes as high as $4 \cdot 10^7$ muons/spill.

Two other targets differ only in plate material. There will be used 20 mm thick stannum plates and 10 mm thick lead plates.

With heavy target modules placed in the beam in front of the hadron calorimeter as shown in fig. 17 the BCDMS spectrometer does not use the target modules inside iron toroids. On the other hand all its 40 m construction is indespensible for triggering the set up by high x events.

4.3. Apparatus Resolution Near $x = 1$

Using of the magnetic spectrometer and the hadron calorimeter together provides the resolution $\sigma(\nu)/\nu$ higher than that of each device separately. The resulting accuracy $\sigma(\nu)$ obtained in such a way is shown in fig. 18 by full line. As is seen

the maximum gain corresponds to the range $\nu < 80$ GeV. These results in considerable improvement of the resolution $\sigma(x)/x$ as it is demonstrated by fig. 19. The calculation has been performed by means of Monte-Carlo that used a polinomial form of the nucleon structure function for computations of cross sections: $F_2(x) \sim x^A(1-x)^B$. Such a form suggests $F_2 = 0$ at $x = 1$ and can not be used for calculations of the resolution in the range beyond $x = 1$. In the last case we used in Monte-Carlo calculations an exponential form $F_2 \sim \exp(-x/0.14)$. The results obtained for the standard BCDMS spectrometer and for the proposed set up (provided that the calorimeter resolution is $\sigma(E)/E = 0.8/E^{0.5}$) are shown in fig. 20. Note that in the kinematical range of the proposed study ($Q^2 > 50$ GeV^2, $\nu > 20$ GeV) the resolution $\sigma(x)/x$ for the modified set up is 12-15% independent of x up to $x \sim 2$. Using Monte-Carlo calculations we have estimated a possibility to discriminate between two predictions for the x-dependence of the structure function $F_2(x)$. As the test versions for the structure functions we took $F_2 \sim (1-x)^3$ and $F_2 \sim \exp(-x/0.12)$. These parametrizations are close to those of experimentally determined in the range below $x = 1$. The simulation has been performed both for the present BCDMS spectrometer and for the proposed version of the set up with the resolution $\sigma(x)/x = 12\%$ independent of x. The results are shown in fig. 21. The two hypotheses can be separated when the differences between event rates uncorrected for resolution exceed by a factor of 3 the experimental errors in corresponding x-bins. For the version with a calorimeter this becomes possible already at $x = 0.9 - 1.0$.

5. CONCLUSIONS

The proposed measurements of deep inelastic scattering of muons on nuclei at $0.5 < x < 2$ and $50 < Q^2 < 200$ are going to yield for the first time high statistics data on nucleon structure functions around single nucleon kinematic limit. The analysis will be free of uncertainties due to errors in $R = \sigma_L / \sigma_T$ [32] that is known to be negligibly small in the kinematic range of the study. The latter is also important for the measurements of structure function ratios F_2^A/F_2^D with small systematic errors. The data to be obtained in the $x < 1$ range will help to clarify the situation with explaining the EMC effect since many models differ significantly in this very region.

At last the proposed experiment can be considered as a crucial test of an existence of multi-quark configurations in a nucleus. It will also test such models as a few nucleon correlation model and a quark-parton model that predict specific behaviour of a nucleon structure function beyond single nucleon kinematic limit.

6. ORGANIZATION MATTERS

Physicists from JINR (Dubna), Lebedev Physical Institute (Moscow) and ITEP (Moscow) intend to carry out the proposed experiment. They are ready to prepare the hadron calorimeter and the targets for this measurement and participate in the setting up, data taking and analysis. For more effective work at two last stages of the experiment the participation of physicists from CERN memberstates are desirable. We are involved now in a search of such participants.

Previous participants of the NA-4 collaboration from Institute di Fisica dell'Universita and INFN, Bologna, Section Physik der Universität, Munich and from CEN, Saclay have kindly permitted the use of belonging to them apparatus by the new collaboration built around the proposed experiment. We would like to ask for permission to use also the NA-4equipment belonging to CERN.

Some financial and technical support of the CERN EP devision is needed for running and maintenance of the apparatus as well as the service in the runs on deuterium targets.

Table 1

Running Time

Target	Days	Usefull muons
D_2	60	$6.3 \cdot 10^{12}$
N_2	28	$2.9 \cdot 10^{12}$
Al (1 m)	28	$2.9 \cdot 10^{12}$
Fe	35	$5.4 \cdot 10^{12}$
Sn	28	$2.9 \cdot 10^{12}$
Pb	14	$1.47 \cdot 10^{12}$
Calibrations	7	π - beam
Total	200	

REFERENCES

1. D. Bollini et al. Nucl.Instr. and Methods 226(1984), 330.
2. J.J. Aubert et al. Phys.Lett. 123B(1983), 275.
3. C. Llewellyn-Smith. Proceedings of the 10-th Int.Conf. on Particles and Nuclei, Heidelberg 1984.
4. N.N. Nikolaev, Proceedings of the 7-th Int.Seminar on HEP Problems, Dubna 1984, p.144.
5. D. Allasia et al. CERN/SPSC 85-18, Febr. 1985.
6. A.C. Benvenuti et al. Report at the 20-th Rencontre de Moriond, Les Arcs, France, March 1985.
7. R.G. Arnold et al. Phys.Rev.Lett 52(1984), 727.
8. I.A. Savin, G.I. Smirnov. JINR Rapid Communications 2-83, p.3(1983).
9. R.L. Jaffe. Phys.Rev.Lett 50(1983), 228;
   L.L. Frankfurt, M.I. Strikman. Preprint LNPI-886, 1983;
   E.M. Levin, M.G. Ryskin. Preprint LNPI-888, 1983;
   M. Staszel, J. Rozynek, G. Wilk. Preprint IFT 19/83, Warsaw, 1983.
10. F.E. Close, R.G. Roberts, G.G. Ross. Phys.Lett. 129B(1983),346;
    D. Nachtmann, H.J. Pirner. Preprint HD-THEP-83-8, Heidelberg, 1983.
11. J. Swed. Phys.Lett. 128B(1983), 245.
12. C.H. Llewellin Smith. Phys.Lett. 128B(1983), 107;
    M. Ericson, A.W. Thomas. Phys.Lett. 128B(1983), 112;
    A.I. Titov. JINR preprint E2-83-460, Dubna 1983.
13. R.L. Jaffe. Phys.Rev.Lett. 50(1983), 228;
    C.E. Carlson. T.J. Havens. Phys.Rev.Lett. 51(1983), 261;
    H.J. Pirner, J.P. Vary. Preprint UNI-HD-83-02;
    H. Faissner, B.R. Kim. Phys.Lett. 130(1983), 321;
    M. Chemtob, R. Peschanski. Preprint DPh-T/83/116, Saclay 1983;
    S. Data, A. Nakamura. Progr.Theor.Phys. 69(1983), 565, ibid 70(1983), 1682.
14. L.A. Kondratyuk, M. Shmatikov. ITEP Preprints 114(1983) and 13(1984), Moscow.
15. A.V. Efremov, E.A. Bondarchenko. Preprint JINR E2-84-124, Dubna 1984.
16. S. Gupta, K.V.L. Sarma. Preprint TIFR/TH/85-4, Bombey 1985.
17. A. Devoto, D.W. Duke, J.F. Owens. PhysRev. D27(1983), 508.

18. L.L. Frankfurt, M.I. Strickman. Phys.Rep . 76(1981), 215.
19. A.V. Efremov, Particles and Nuclei, 13(1982), 613.
20. A.V. Efremov. Sov.Jorn.Nucl.Phys. 34(6)1208. 1976.
21. A.M. Baldin. JINR Reports, E2-83-415, Dubna 1983.
22. A.M. Baldin. Particles and Nuclei, 8(1977), 429.
23. V.S. Stavinsky. Particles and Nuclei, 10(1979), 950.
24. A.M. Baldin et al. JINR Reports, E2-82-412, Dubna 1982.
25. A.M. Baldin, Yu.A. Panibratsev, V.S. Stavinsky. JINR Reports, 1-84-185, Dubna, 1984.
26. A. Argento et al. The report at the Conf. High Energy Phys. and Nuclear Structure, Versailles, 1981.
27. UA1 Collab., G. Arnison et al. Phys.Lett. 136B(1984), 294.
28. UA2 Collab., P. Bagnaia et al. Phys.Lett. 144B(1984), 283.
29. D. Bollini et al. Nucl.Instr.Meth. 204(1983), 333.
30. L.L. Frankfurt, M.I. Strikman. Preprint LNPI-886, Leningrad, 1983.
31. S.V. Akulinichev, S.A. Kulagin, G.M. Vagradov. Preprint NBI-85-08, Copenhagen, 1985.
32. I.A. Savin. In Proceedings of the XXIInd International Conference on High Energy Physics, Leipzig, July 19-25, 1984. Edited by A. Meyer and E. Wieczorek, Zeuthen, 1984, Volume II, p.251.

FIGURE CAPTIONS

Fig.1. The nucleon structure functions ratio F_2^{Fe}/F_2^D obtained in high energy muon experiments. Dashed area shows predictions that took into account the effect of nucleon Fermi-motion.

Fig.2. The ratio F_2^N/F_2^D as obtained by the BCDMS /6/ compared to the ratio σ^C/σ^D (SLAC /7/).

Fig.3. The ratio of nucleon structure functions measured on iron and deuterium nuclei calculated by different approaches: J.S. /11/, F-S /30/, B-E /15/, K-S(a,b,c,d) /14/ and A-K-V /31/. The statistical accuracy expected in the proposed experiment is shown by the points with error bars.

Fig.4. Ratios σ^A/σ^D (SLAC /7/) and F_2^A/F_2^D (BCDMS /6/) as a function of nuclear weight A.

Fig.5. Predictions for the rate in the deep inelastic muon-iron scattering beyond single nucleon kinematic limit:

a) the dashed line corresponds to the nucleon Fermi--motion model with k_F= 190 MeV;

b) The curve B-E is obtained assuming the existence of quark-parton configurations in a nucleus /15/;

c) the shaded area is restricted by the exponentials $\exp(-x/b)$ with b = 0.105 /27/ and b = 0.12 /28/. Predictions of a few nucleon correlations model /18/ lie within the area.

Fig.6. Results of measurements of the structure functions by methods of a relativistic nuclear physics /25/ along with those obtained in muon and electron deep inelastic scattering.

Fig.7. A-dependence of cross-section ratios at x = 1.3 obtained in experiments on limiting fragmentation /25/. The result is to be checked in deep inelastic scattering of muons on nuclei.

Fig.8. Preliminary results on $F_2^A(x)$ structure function measured by the BCDMS on a carbon target /26/. The solid line is obtained by extrapolating to x=1 $F_2(x)$ measured for $x < 0.7$ assuming $F_2(x) \sim x^A(1-x)^B$.

Fig.9. The layout of the BCDMS spectrometer in the present configuration.

Fig.10. Kinematical diagram of Q^2 vs ν for deep inelastic muon scattering at 200 GeV beam energy. The area shaded by horizontal lines corresponds to the region already explored and by vertical lines to that to be studied.

Fig.11. Effect of suppression of low x events by first level trigger demonstrated on experimental events registered by the front set up of the BCDMS spectrometer. Number of muons with particular value of x traversing 4, 8, 10 or 12 trigger counter planes are shown by different symbols as a function of x.

Fig.12. Selection efficiency of the events in the range $x > 0.6$ as a function of the P_T cut with respect to the number of events at $x > 0.6$ (solid line, left scale) and with respect to all events (dashed line, right scale).

Fig.13. Vertex distribution for the events registered on D_2 at 280 GeV as a function of the target length. The arrows indicate the targets ends.

Fig.14. Statistical accuracy in the expected ratio of nitrogen to deuterium structure functions (closed points) compared to that already awailable from the BCDMS (open points).

Fig.15. Front part of the modified BCDMS spectrometer equiped with an hadron calorimeter (HC).

Fig.16. Acceptance of the calorimeter as a function of a distance to the vertex. The calorimeters with dimensions 3×3 m^2 and 3×1.5 m^2 at $z = 15$ m have beam used in simulation.

Fig.17. The target configuration for heavy targets runs.

Fig.18. Accuracy $\sigma(\nu)$ in hadron shower energy measurements as it is determined by the magnetic spectrometer and the calorimeter separately (dashed lines) and by their joint use (solid line).

Fig.19. The resolution $\sigma(x)$ of the BCDMS spectrometer as a function of Q^2 for various x-bins in present configuration (solid lines) and together with a calorimeter (dashed lines) with $\sigma(E)/E = 0.8/E^{0.5}$.

Fig.20. Resolution $\sigma(x)/x$ of the present BCDMS spectrometer as a function of x in a wide x-range (open points) and of the spectrometer with a calorimeter (closed points).

Fig.21. Full lines demonstrate differences between uncorrected for smearing event rates due to different $F_2(x)$ parametrizations. The differences show up for higher x in the case of larger smearing (T NA-4).

The statistical errors in the corresponding bins are shown for the already available statistics (dashed line) and for the estimated statistics in 25 days run on iron (dashed dotted line).

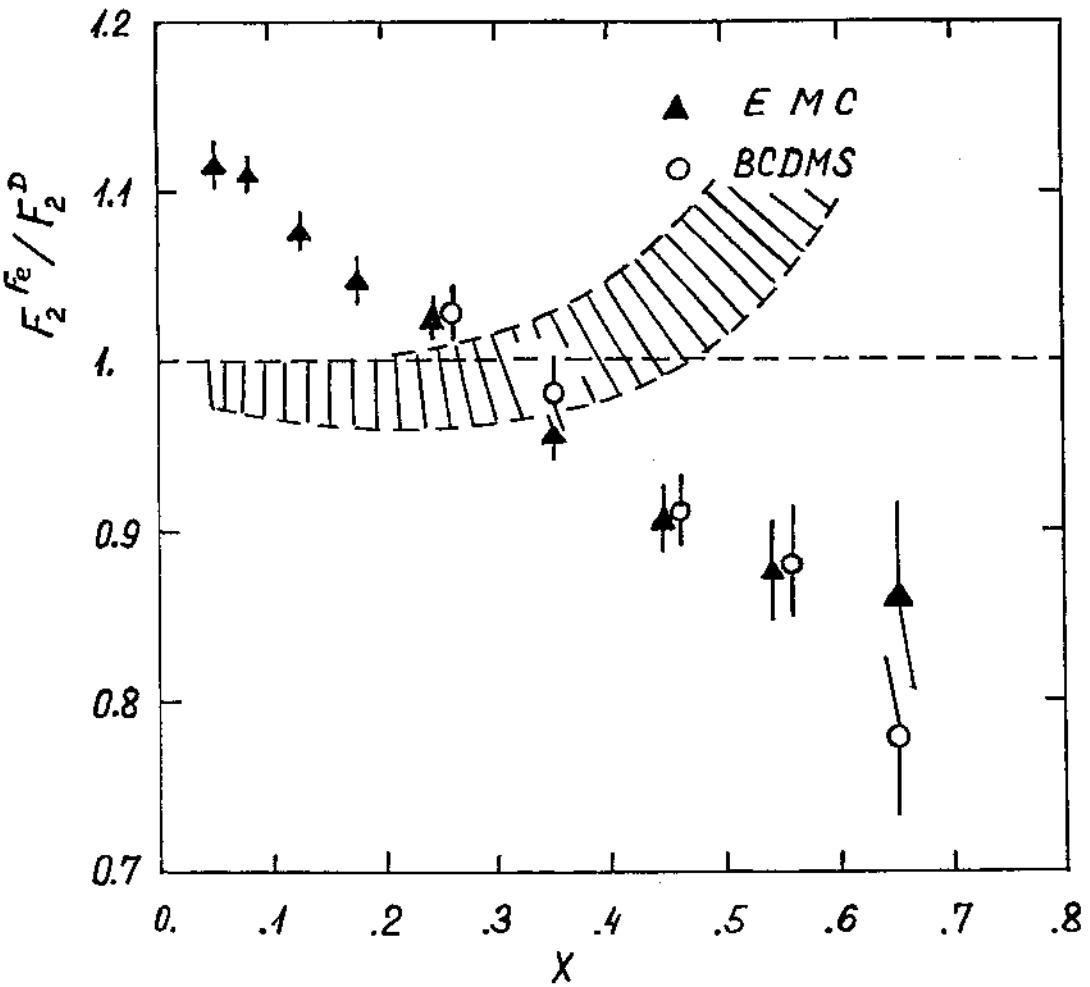

Fig. 1

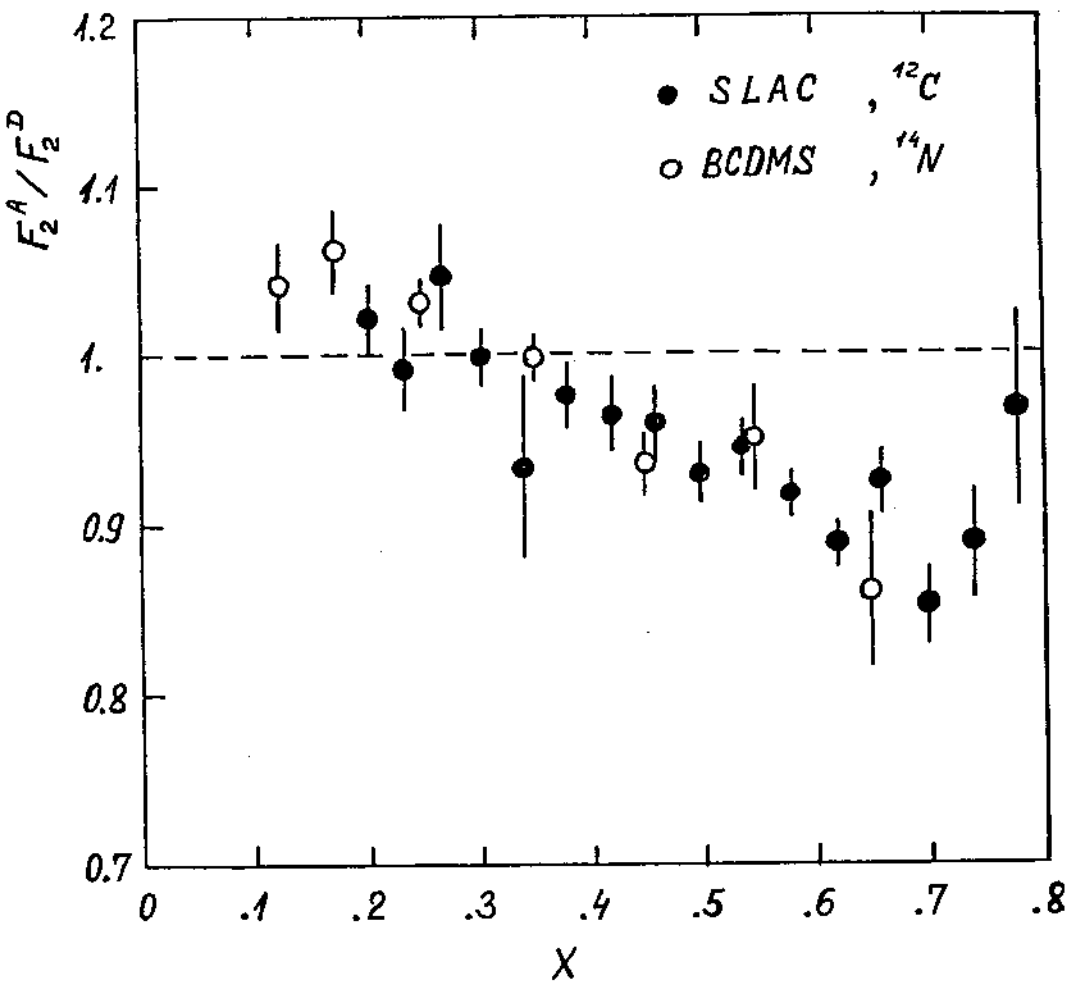

Fig. 2

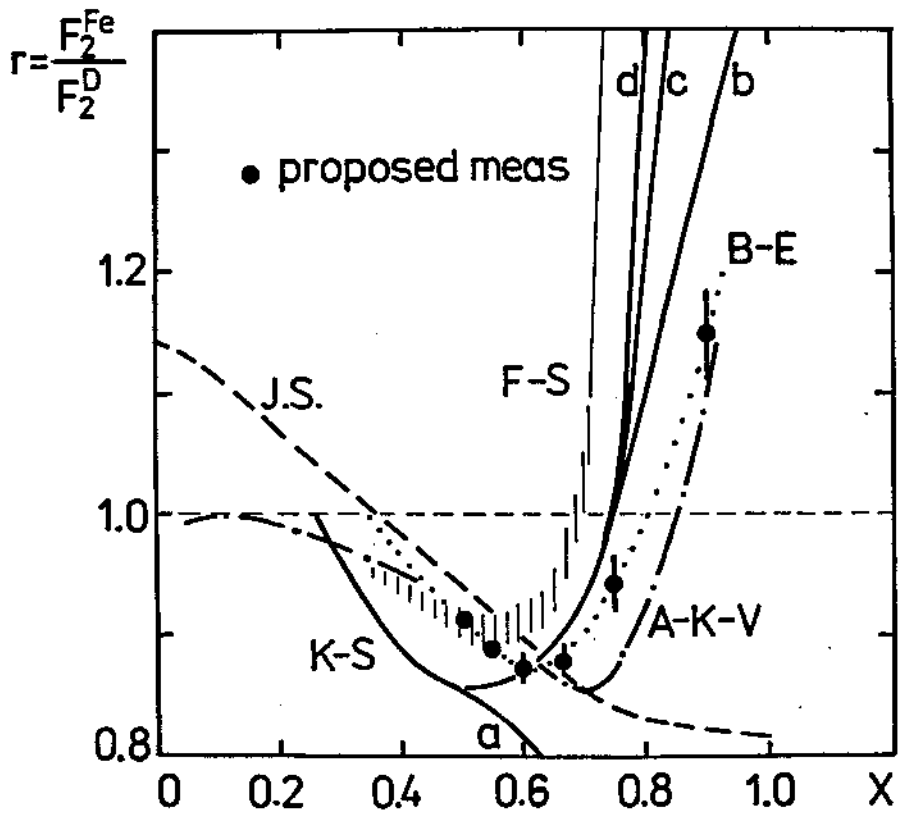
r=F2Fe/F2D
proposed meas
d
c
b
B-E
J.S.
F-S
A-K-V
K-S
a
1.2
1.0
0.8
0
0.2
0.4
0.6
0.8
1.0
X

Fig. 3

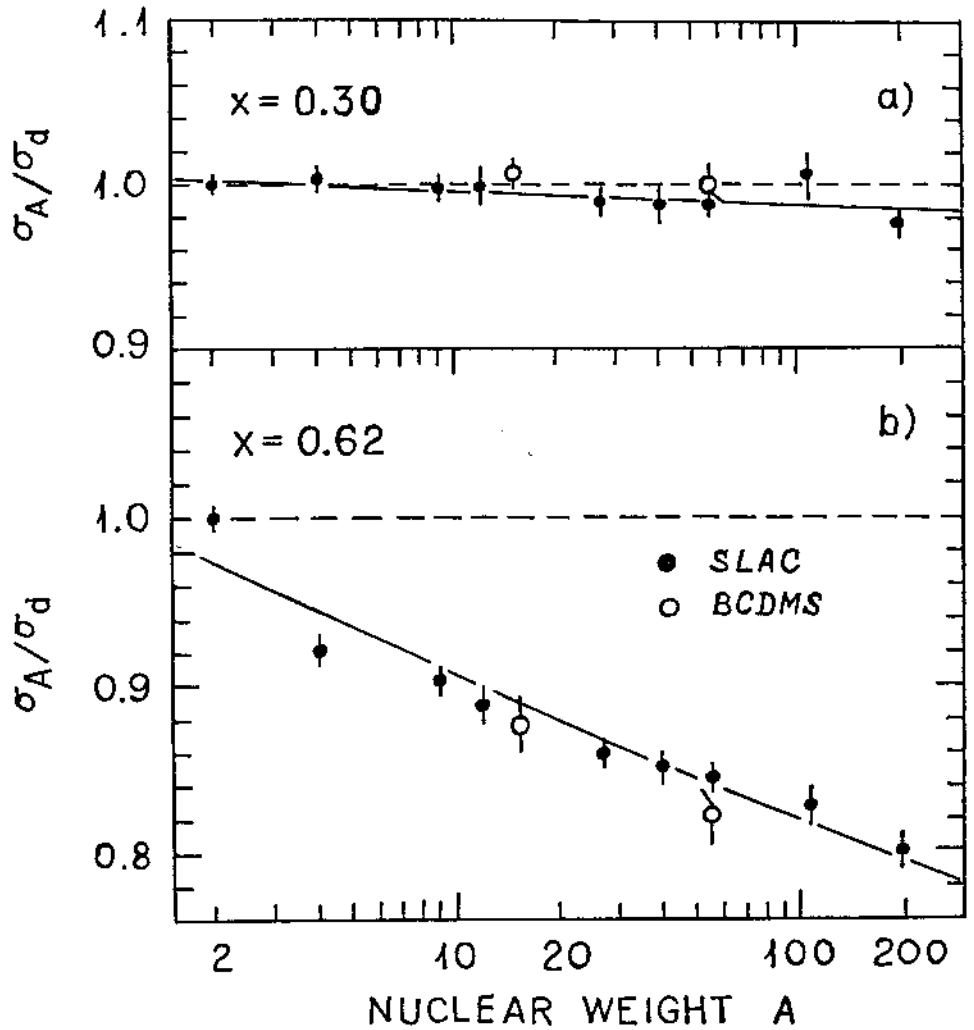
1.1
1.0
0.9
x = 0.30
a)
σ_A/σ_d
x = 0.62
b)
1.0
0.9
0.8
SLAC
BCDMS
2
10
20
100
200
NUCLEAR WEIGHT A

Fig. 4

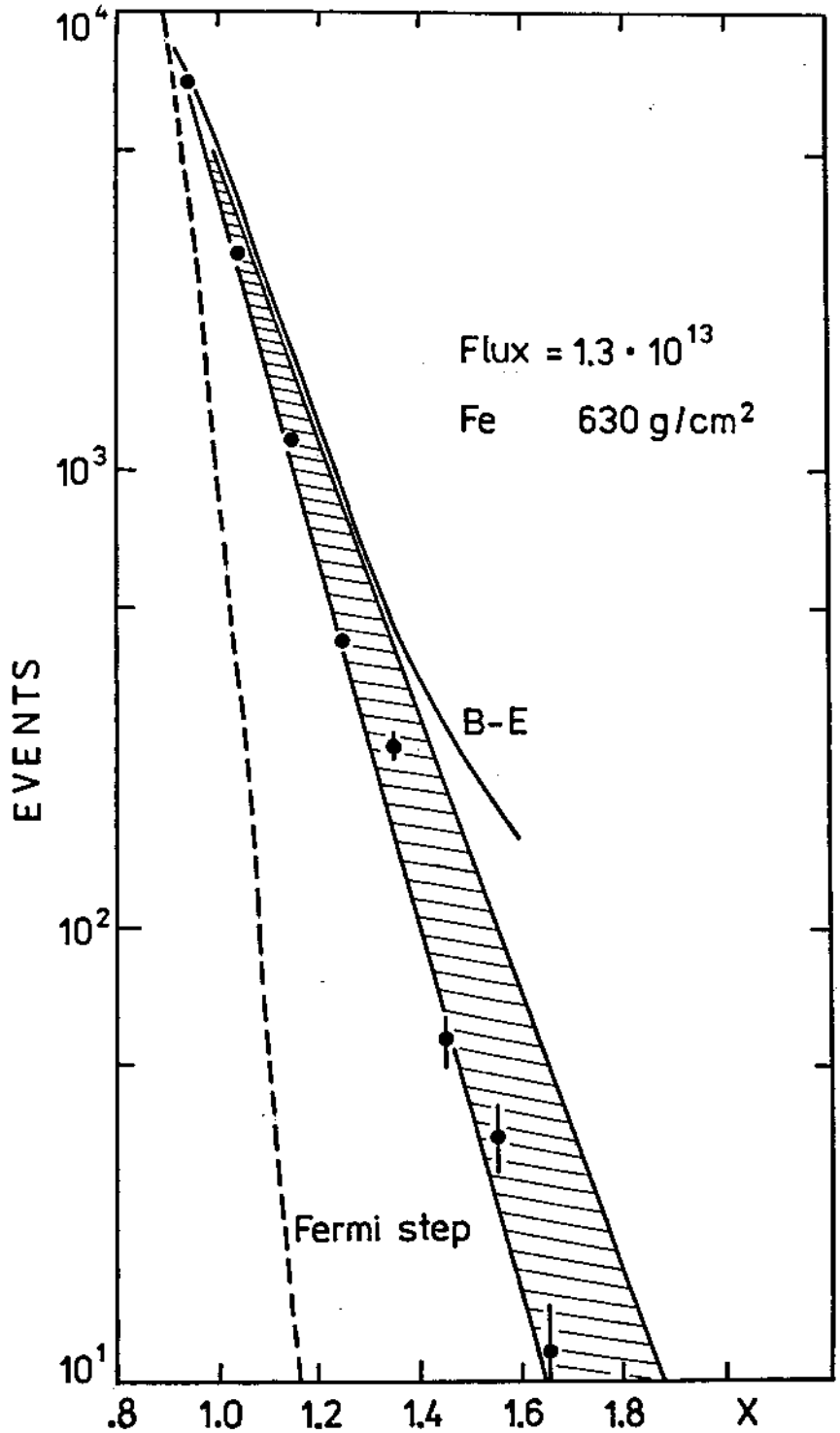
10^4
10^3
10^2
10^1
EVENTS
Flux = $1.3 \cdot 10^{13}$
Fe 630 g/cm^2
B-E
Fermi step
.8
1.0
1.2
1.4
1.6
1.8
X

Fig. 5

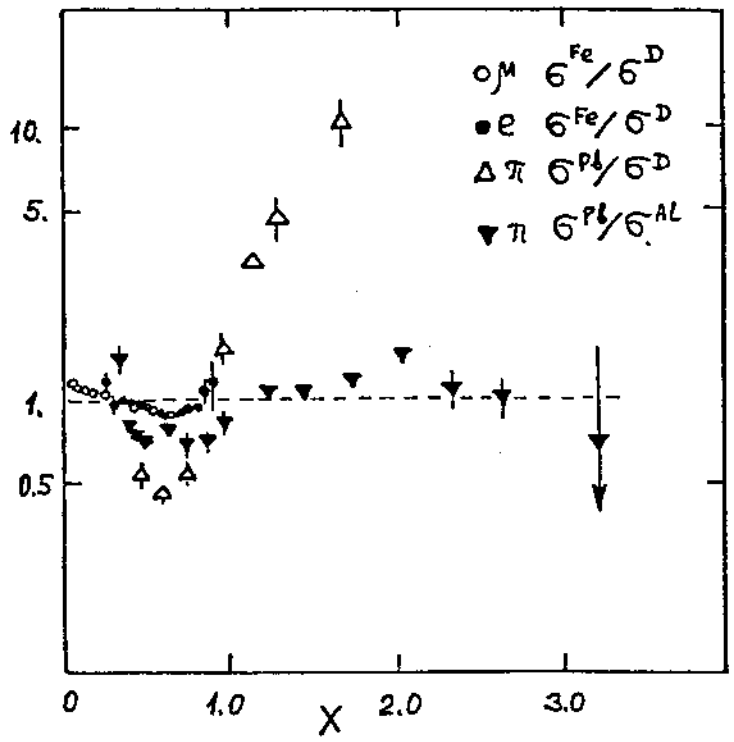
○μ σ^Fe/σ^D
● e σ^Fe/σ^D
△ π σ^Pb/σ^D
▼ π σ^Pb/σ^AL
10.
5.
1.
0.5
0
1.0
X
2.0
3.0

Fig. 6

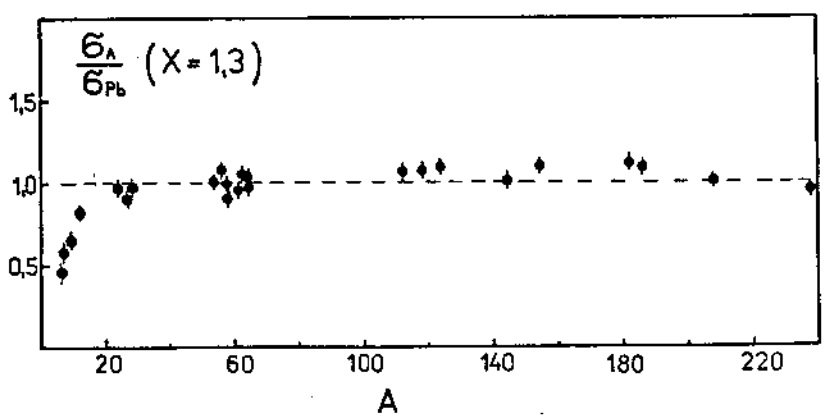
σ_A/σ_Pb (X = 1,3)
1,5
1,0
0,5
20
60
100
140
180
220
A

Fig. 7

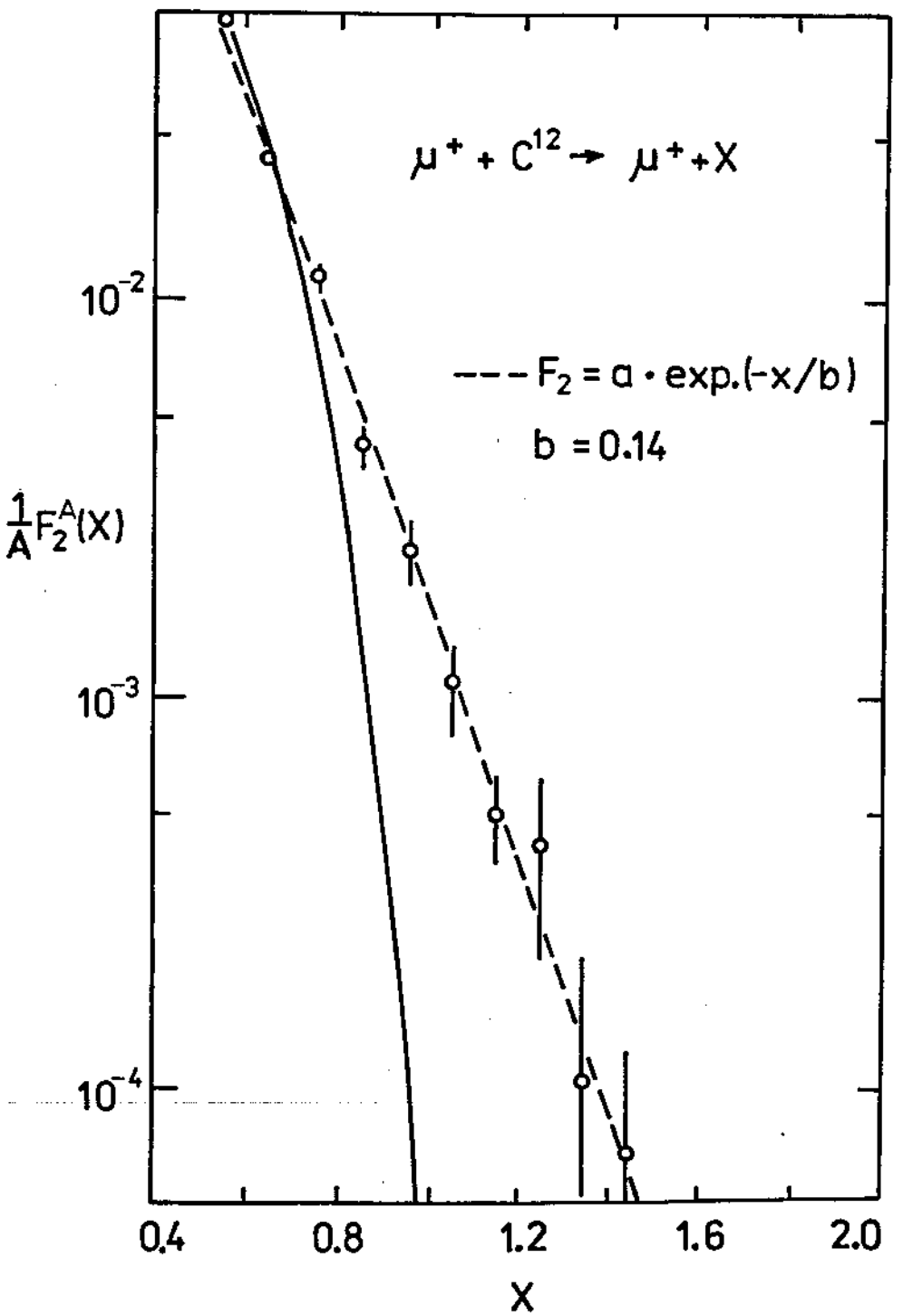
$\mu^+ + C^{12} \rightarrow \mu^+ + X$
$--- F_2 = a \cdot \exp.(-x/b)$
$b = 0.14$
$\frac{1}{A}F_2^A(X)$
10^{-2}
10^{-3}
10^{-4}
0.4
0.8
1.2
1.6
2.0
X

Fig. 8

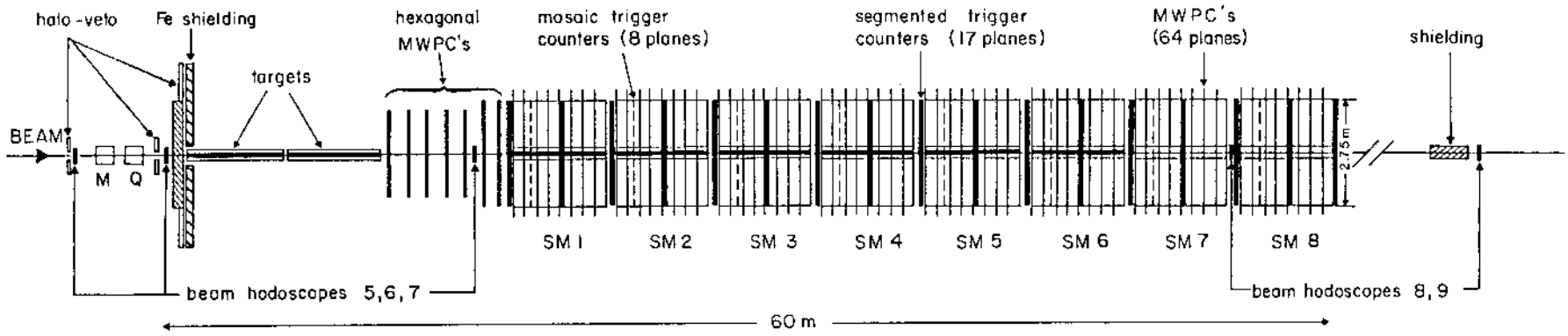
halo-veto
Fe shielding
targets
hexagonal MWPC's
mosaic trigger counters (8 planes)
segmented trigger counters (17 planes)
MWPC's (64 planes)
shielding
BEAM
M
Q
SM 1
SM 2
SM 3
SM 4
SM 5
SM 6
SM 7
SM 8
2.75 m
beam hodoscopes 5,6,7
beam hodoscopes 8,9
60 m

Fig. 9

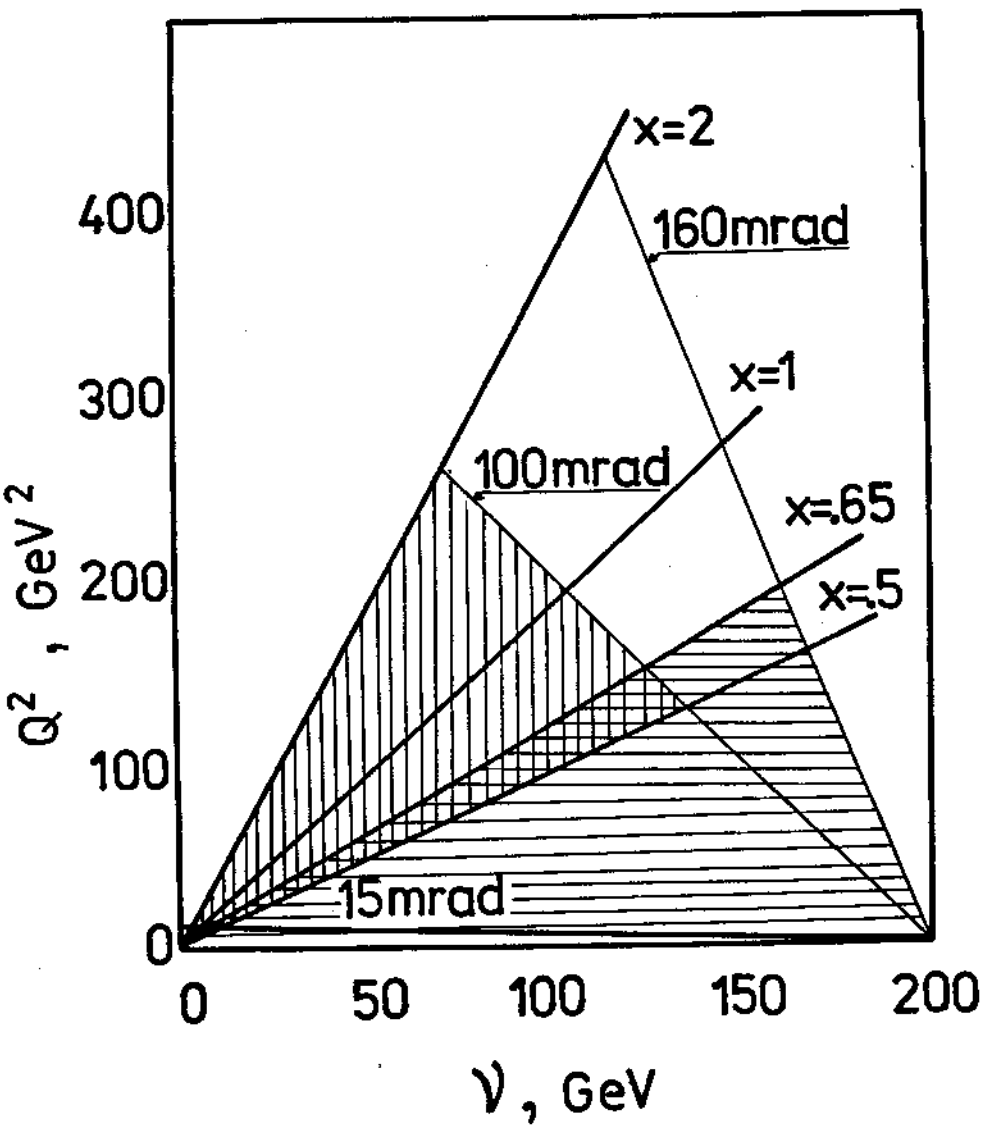
x=2
160mrad
x=1
100mrad
x=.65
x=.5
15mrad
400
300
200
100
0
Q^2 , GeV^2
0
50
100
150
200
ν , GeV

Fig.10

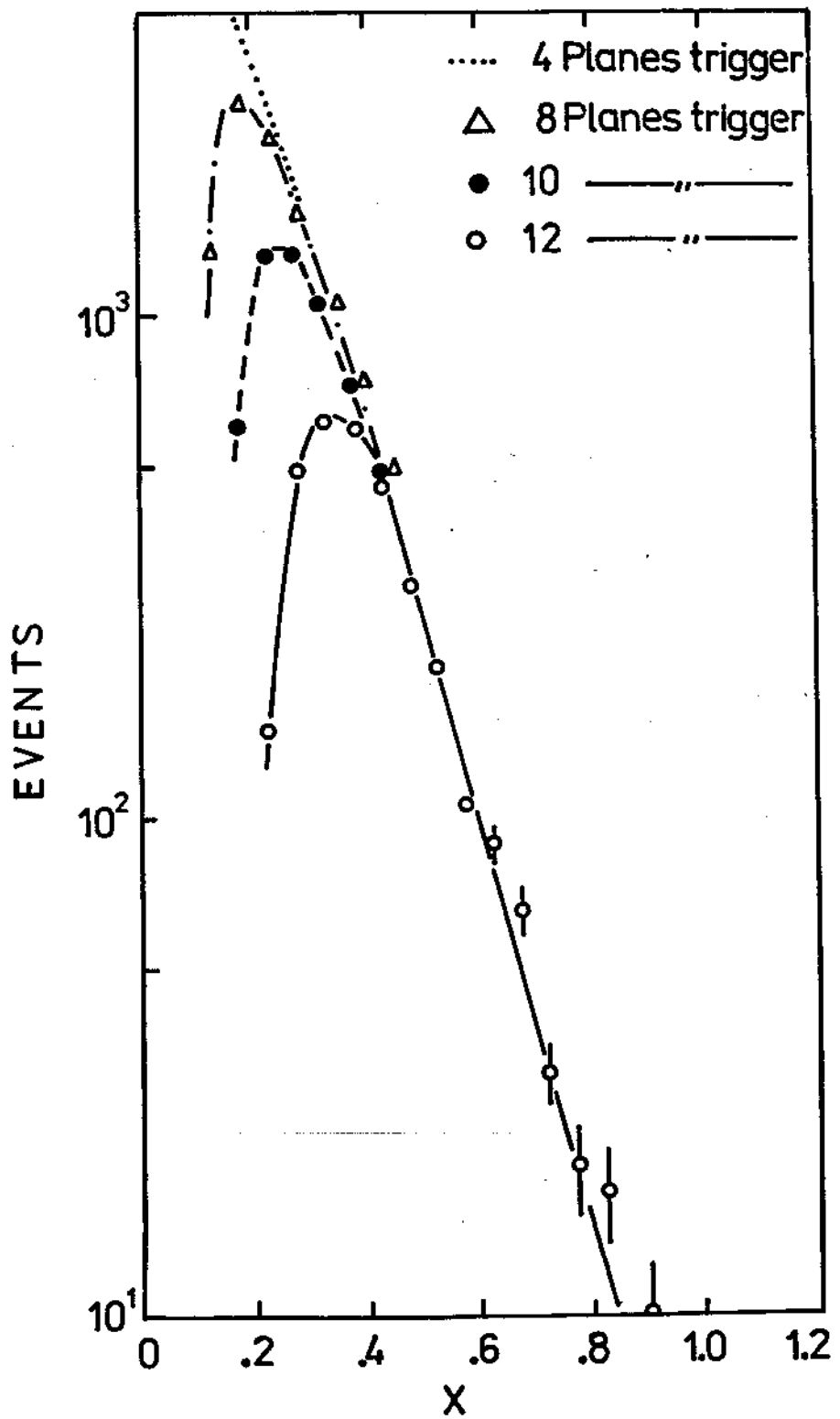
4 Planes trigger
8 Planes trigger
10
12
EVENTS
10^3
10^2
10^1
0
.2
.4
.6
.8
1.0
1.2
X

Fig. 11

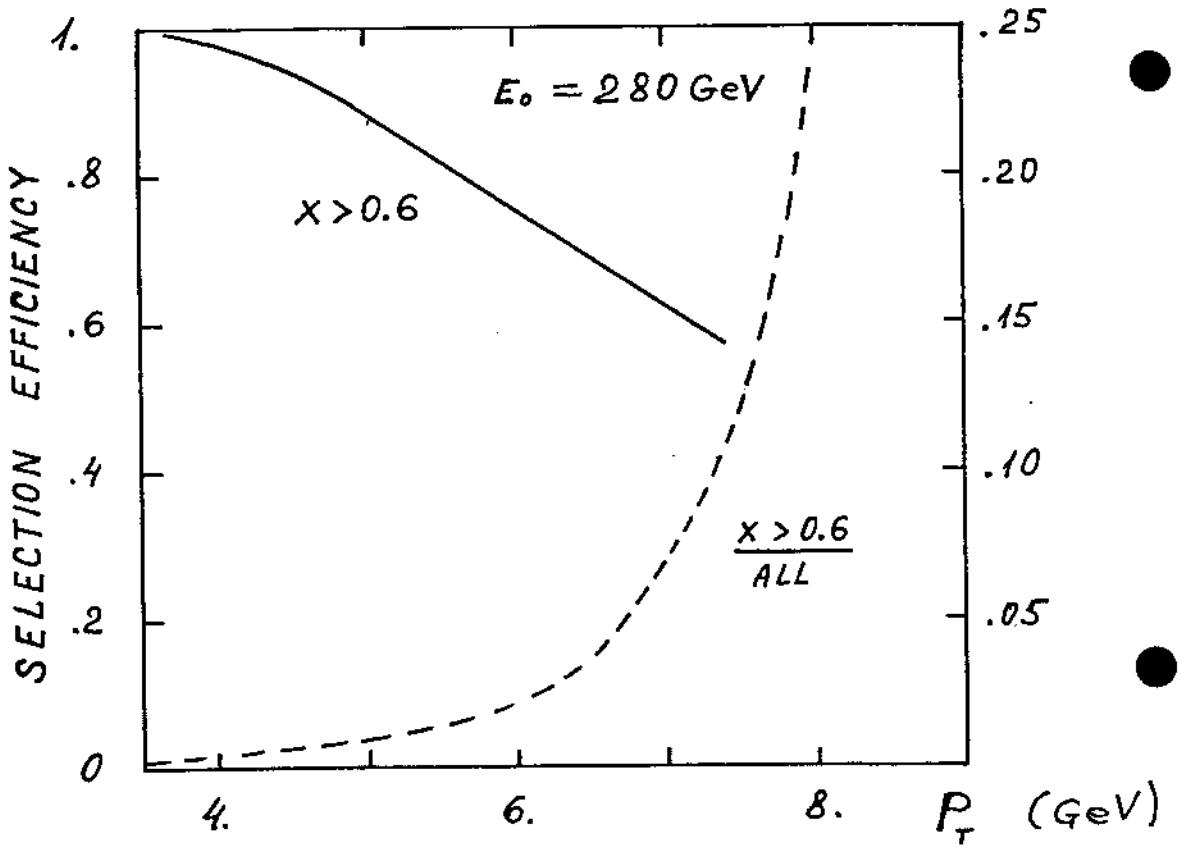
1.
.8
.6
.4
.2
0
SELECTION EFFICIENCY
.25
.20
.15
.10
.05
$E_0 = 280$ GeV
X > 0.6
X > 0.6 / ALL
4.
6.
8.
P_T (GeV)

Fig. 12

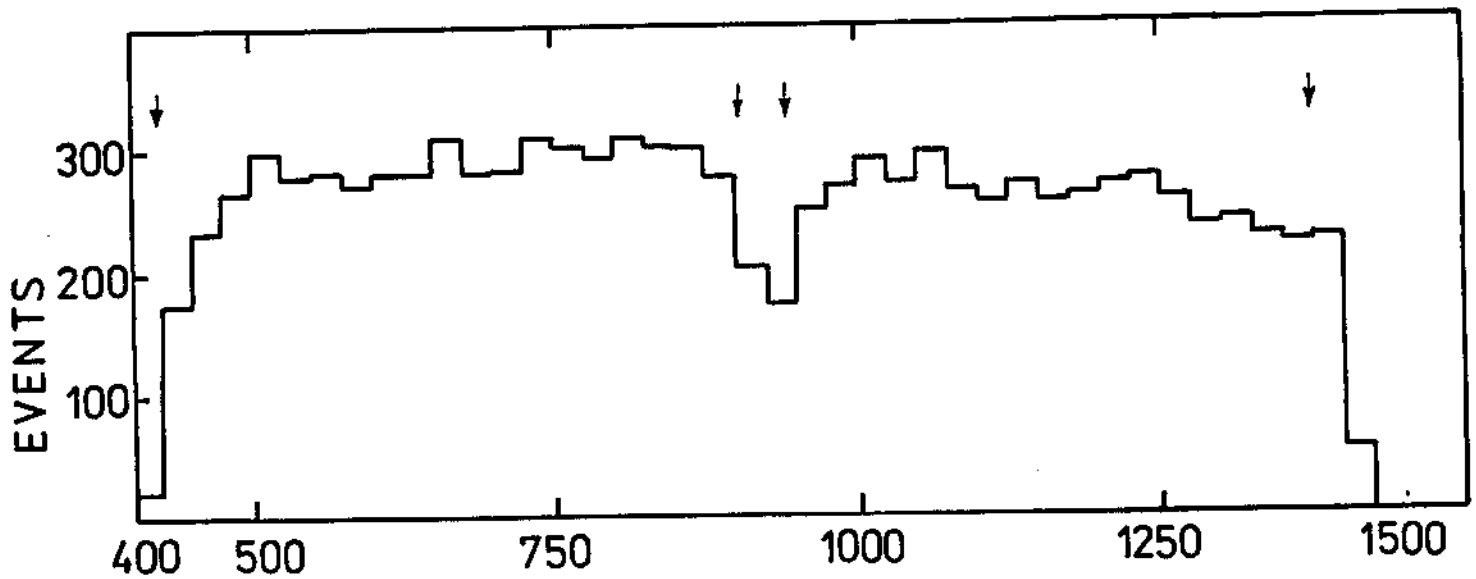

Fig. 13

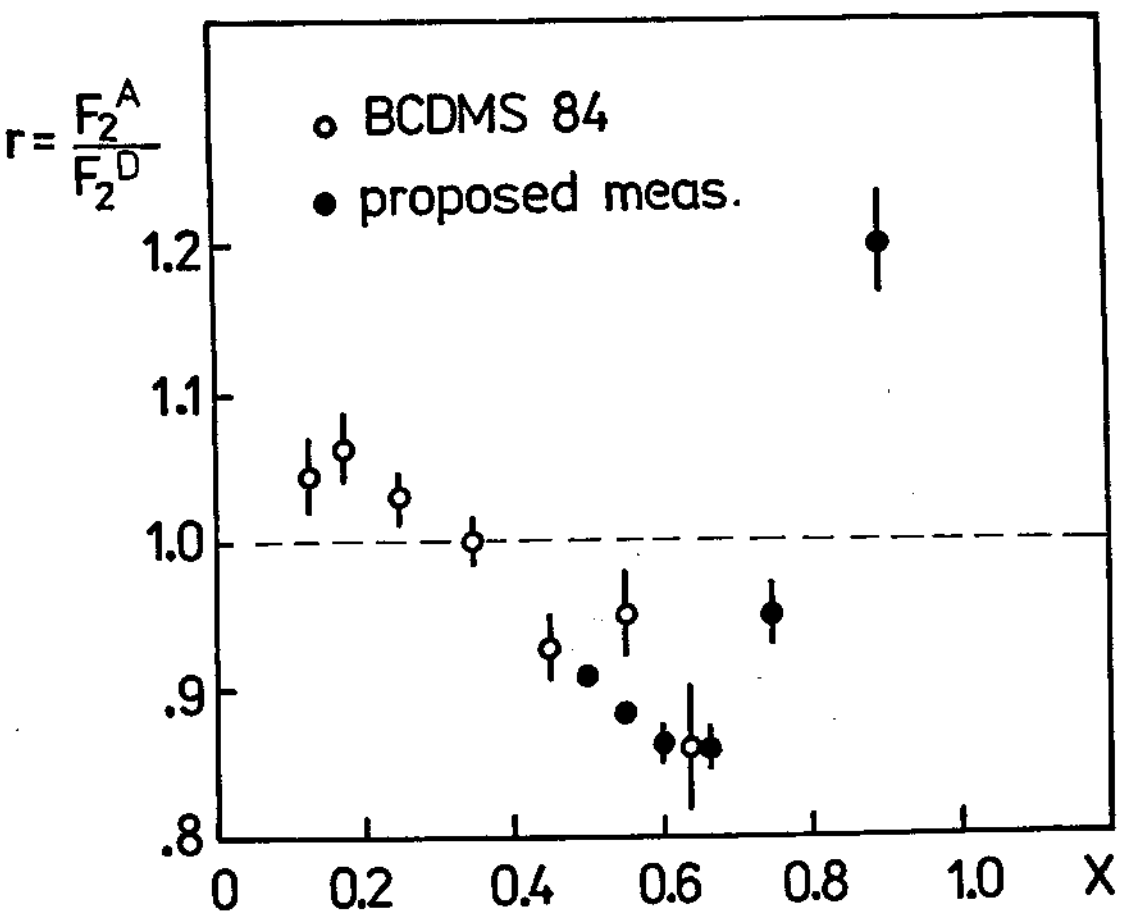

Fig. 14

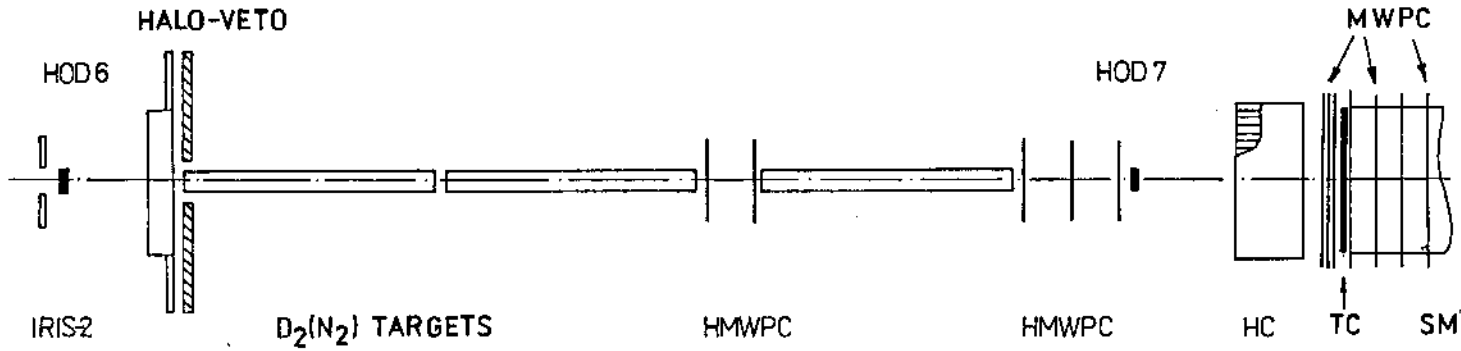
HALO-VETO
HOD 6
HOD 7
MWPC
IRIS-2
$D_2(N_2)$ TARGETS
HMWPC
HMWPC
HC
TC
SM

Fig.15

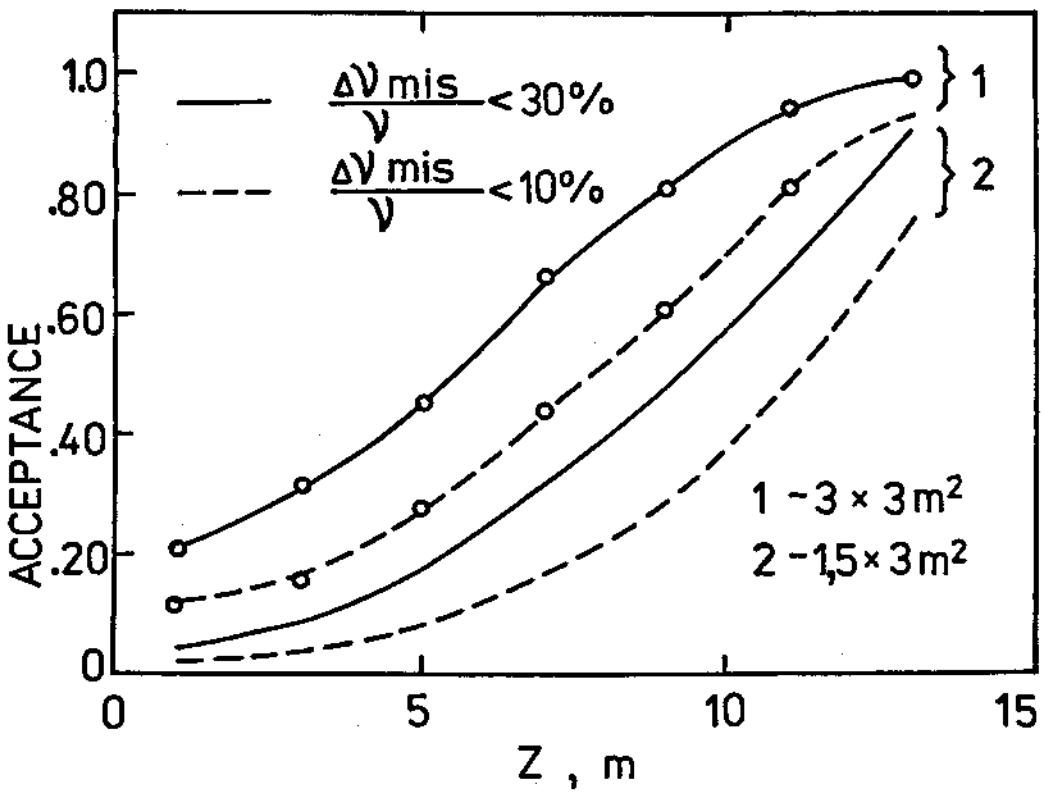
1.0
.80
.60
.40
.20
0
ACCEPTANCE
Δν mis / ν < 30%
Δν mis / ν < 10%
1
2
1 - 3 × 3 m²
2 - 1,5 × 3 m²
0
5
10
15
Z , m

Fig. 16

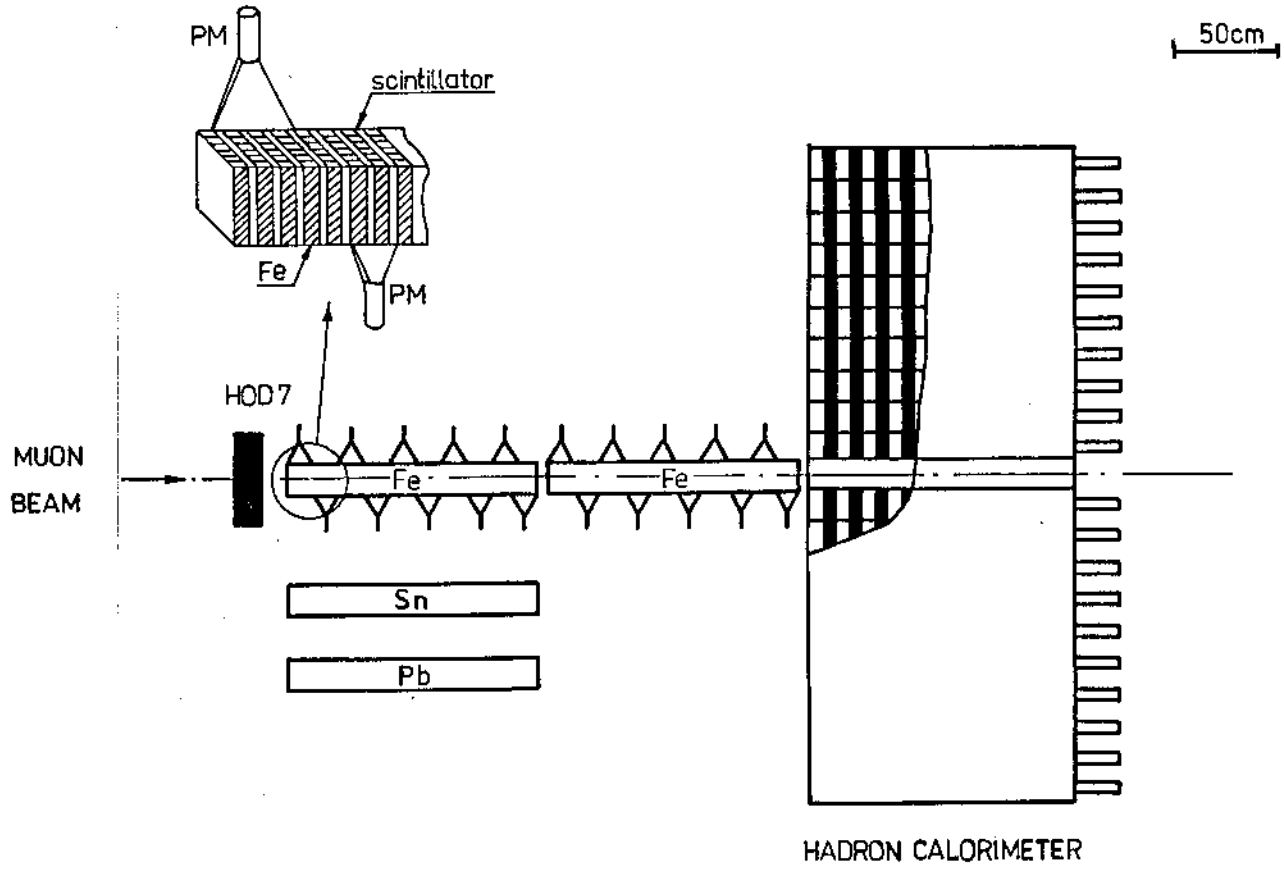
PM
scintillator
Fe
PM
50cm
HOD7
MUON
BEAM
Fe
Fe
Sn
Pb
HADRON CALORIMETER

Fig.17

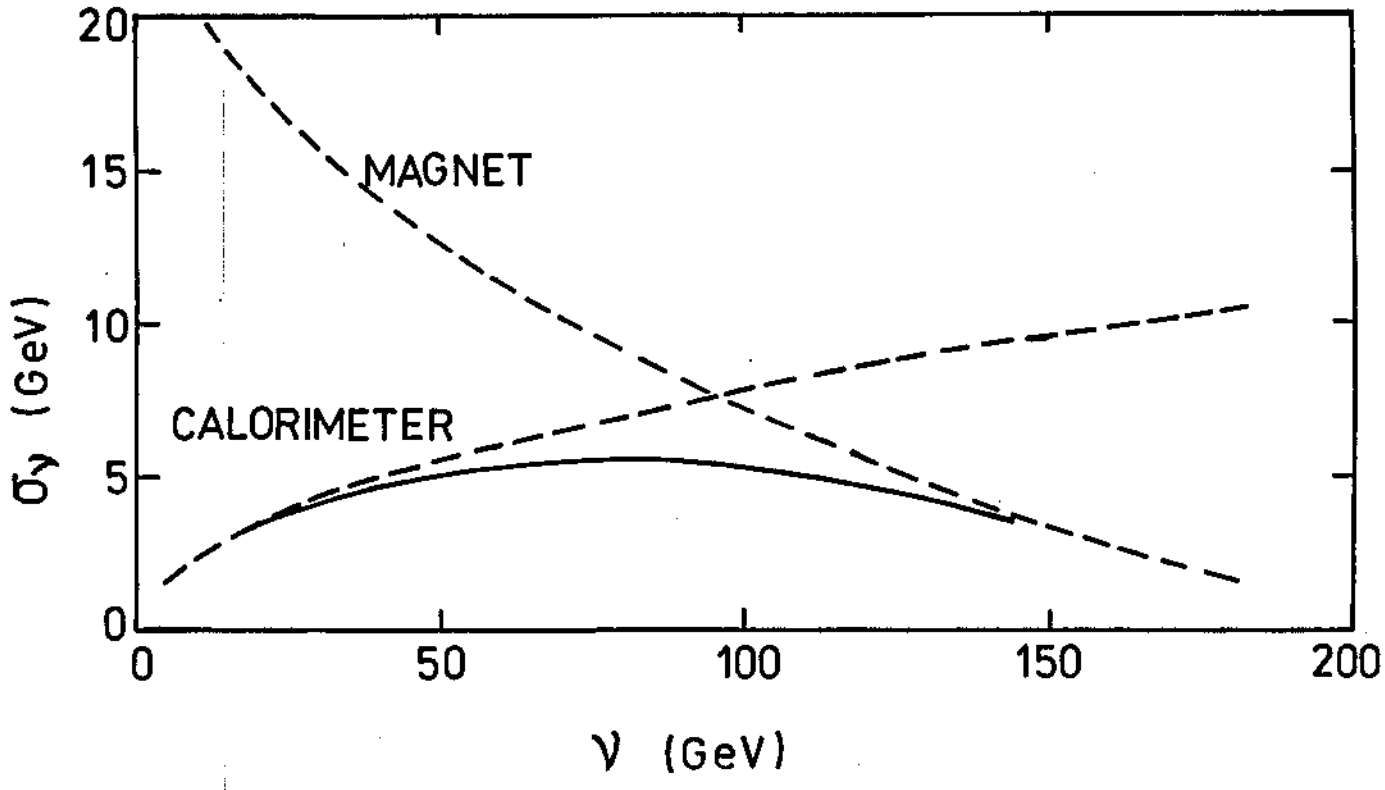
20
15
10
5
0
0
50
100
150
200
MAGNET
CALORIMETER
σ_y (GeV)
ν (GeV)

Fig. 18

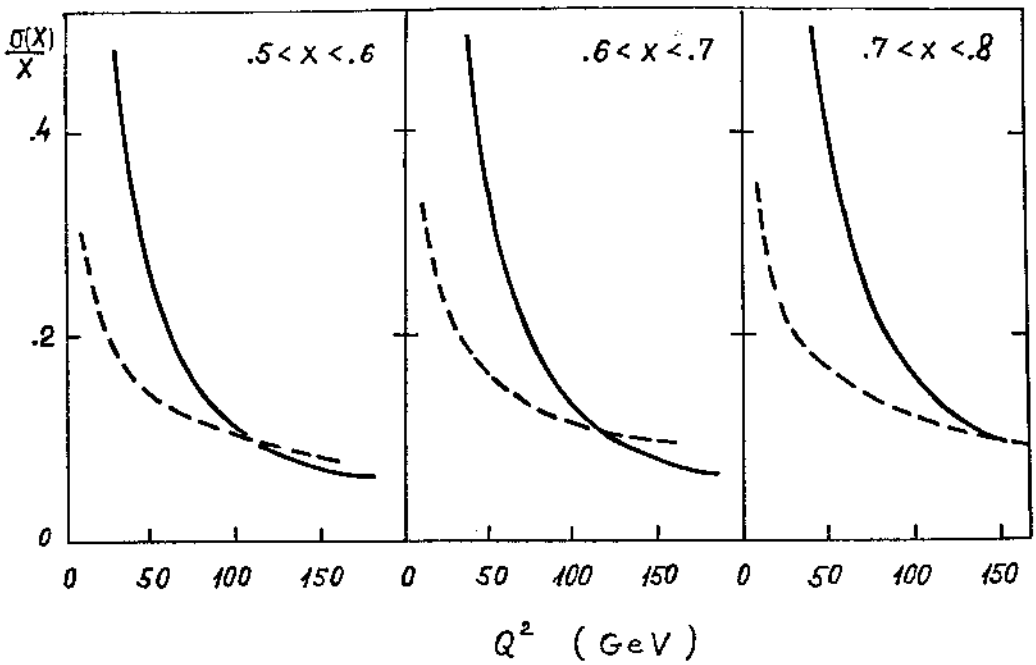
σ(X)/X
.5 < x < .6
.6 < x < .7
.7 < x < .8
.4
.2
0
0
50
100
150
Q² (GeV)

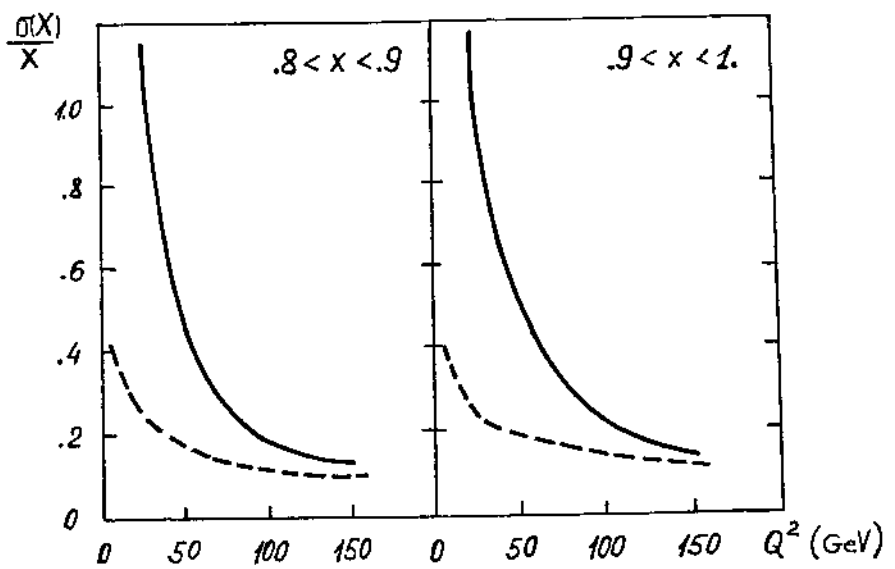
σ(X)/X
.8 < x < .9
.9 < x < 1.
1.0
.8
.6
.4
.2
0
0
50
100
150
Q² (GeV)

Fig.19

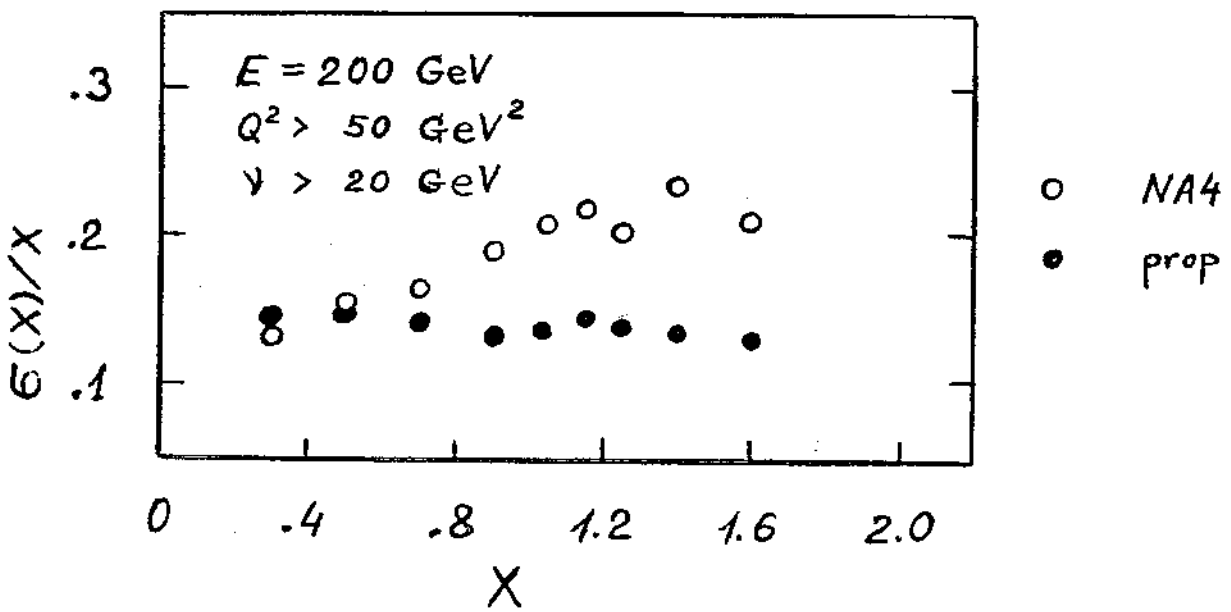

Fig. 20

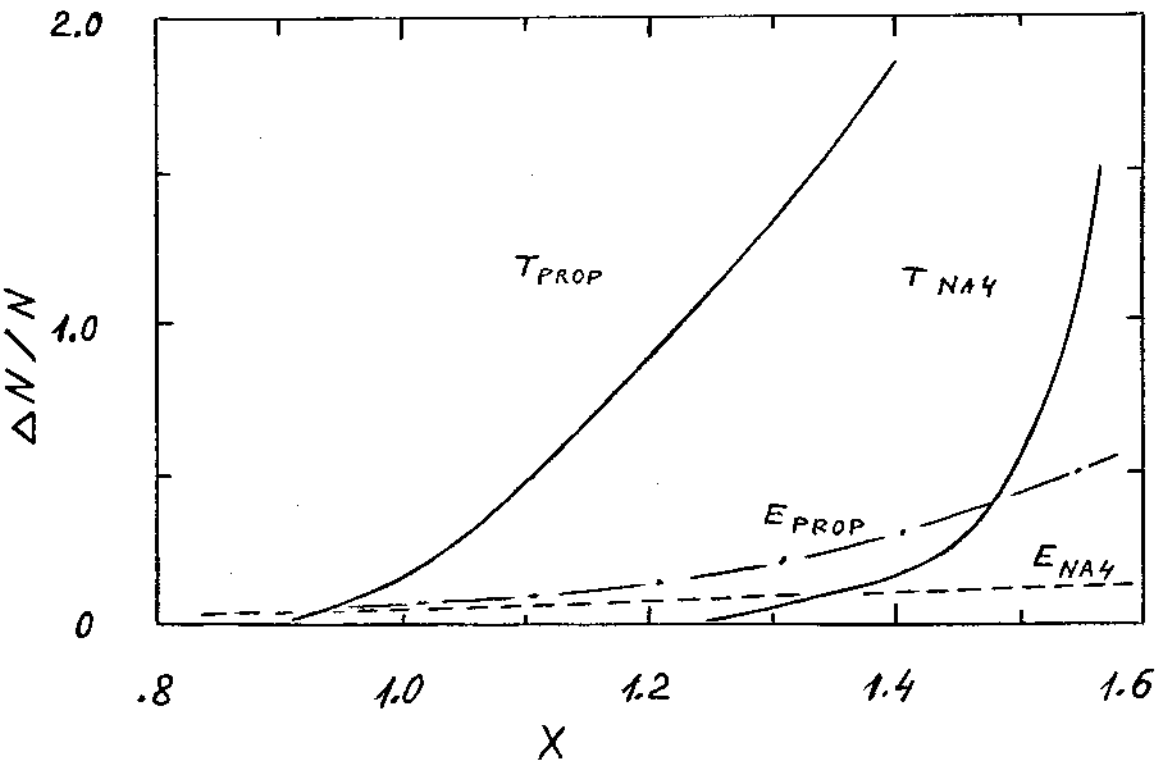

Fig. 21